Formulation and Characterization of Fatigue Strength Diagrams of Notched Specimens Based on Equivalent Cyclic Stress Ratio, Attending Especially to Material Dependence and Notch Size Effects

Hiroshi Matsuno[1,*]

[1] Department of MECHANICAL ENGINEERING, SOJO University, Kumamoto 860-0082, Japan
* Corresponding author: hi-matsuno@par.odn.ne.jp

Abstract In the present paper, a fatigue strength diagram is formulated and characterized as a function of an equivalent cyclic stress ratio (named as R_{EQ}-ratio). The R_{EQ}-ratio is derived from a hypothesis of plastic adaptation that reflects micro-mechanical behavior of a fatigue slip band, and it was proposed as a corresponding parameter between cyclic stress-conditions of notched and un-notched specimens in the previous paper. The R_{EQ}-ratio is given as a function of a theoretical stress concentration factor K_t and a nominal cyclic stress ratio R_N, and it is noteworthy that the R_{EQ}-ratio materializes a similitude relation between the fatigue strength diagrams of notched and un-notched specimens in the case where the notch depth is greater than about 1*mm* (where the notch size effect is negligible). Therefore, the R_{EQ}-ratio can be applied as a main variable to the formulation of the fatigue strength diagram. The formulation is extended to the case of the extremely shallow notch where the size effect is dominant, and finally the generalized equations expressing the fatigue strength diagrams are proposed. These equations are applied to regression analyses on fatigue data of practically used metallic materials. Consequently, the material- and size-dependence in notch effects are considered and characterized.

Keywords Fatigue strength diagram, Cyclic plastic-adaptation, Equivalent cyclic stress ratio (R_{EQ}-ratio), Notch behavior map, Notch size effect

1. Introduction

A fatigue strength diagram is formulated and characterized as a function of an equivalent cyclic stress ratio (named as R_{EQ}-ratio). The R_{EQ}-ratio is derived from a hypothesis of cyclic plastic adaptation that reflects micro-mechanical behavior of a fatigue slip band, and it was proposed as a corresponding parameter between cyclic stress condition of notched and un-notched specimens in the previous paper [1]. A graphic method estimating the R_{EQ}-ratio on the basis of the hypothesis is developed in the present paper. It is described that the R_{EQ}-ratio materializes a similitude relation between the fatigue strength diagrams of the notched and un-notched specimen in the case where the notch depth is comparatively large size of *mm*-order (where the notch size effect is negligible). It means that the R_{EQ}-ratio can be applied as a main variable to the formulation of the fatigue strength diagram. Next, the notch behavior is characterized and mapped by making the notch root radius and depth into variables. The notch size effect is discussed on the basis of the notch behavior map and the size effect factors are introduced. As a result, the formulation of the fatigue strength diagram can be extended to the case of the extremely small size notch, such as the depth of 10 and 100 μm-order, where the size effect is dominant, and finally the generalized equations expressing the fatigue strength diagrams are proposed. These equations are applied to regression analyses on fatigue data of practically used metallic materials.

2. Graphic method estimating an equivalent cyclic stress ratio (R_{EQ}-ratio)

2.1. A hypothesis of cyclic plastic-adaptation

Irreversible microscopic expansion developing in the slip direction of a crystal of a persistent slip

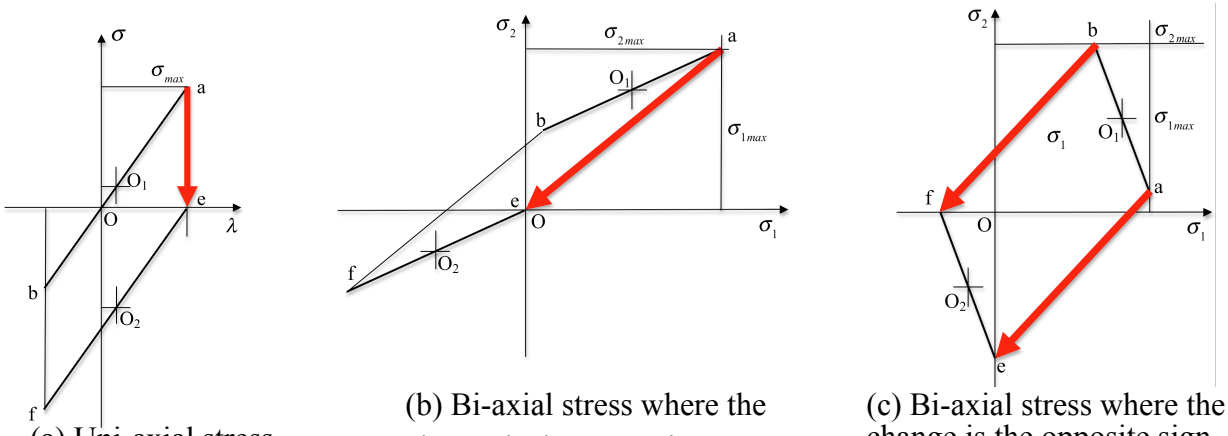

(a) Uni-axial stress (b) Bi-axial stress where the change is the same sign (c) Bi-axial stress where the change is the opposite sign

Fig. 1 Change of the stress path under cyclic plastic-adaptation

band is released on the surface and forms surface relief [2-4]. On the other hand, it is inside restrained and produces inherent compressive stress. A hypothesis that reflects such microscopic mechanical behavior in the persistent slip band is introduced from a viewpoint of macro-mechanics as follows. At the weakest spot of a surface layer, a notch root and a fatigue crack tip, the elastic expansion arising at the maximum stress is transformed into the irreversible expansion inherent in fatigue. As a result, the maximum stress at the weakest spot is substantially decreased and the elastic energy is relieved. Therefore, it is termed as the hypothesis of cyclic plastic-adaptation by author. Such stress relief is materialized for each maximum principal stress in a multi-axial stress condition, too. The expansion arising by the plastic adaptation behaves as a mechanical misfit and lowers the mean stress of substantial cyclic stress. Accordingly, the cyclic behavior of stress can be imaged as shown in Figs. 1(a)-(c). They show the cases of uni-axial stress (a), bi-axial stress where the change is the same (b) and opposite sign (c). At the weakest spot of the surface layer, the stress path moves from a site *ab* to a site *ef*, in common in each figure, though the outward path remains at a site *ab*. The cyclic plastic-adaptation is accomplished completely at the site *ef*. As mentioned later, it should be noted that the movement of the stress path caused by growth of irreversible expansion means not a change of itself but the movement of the potential field that it has.

2.2. Derivation of the equivalent cyclic stress ratio (R_{EQ}-ratio)

How to reproduce the cyclic stress potential field at a notch root as that in the surface layer of the un-notch condition is illustrated based on the hypothesis of cyclic plastic-adaptation. Concretely speaking, the cyclic stress that activates microscopic slip behavior in the un-notch condition as much as the cyclic stress does at the notch root is pictured on the diagram of the stress path. From this diagram, the equivalent cyclic stress ratio R_{EQ} and the equivalent mean stress $\sigma_{mean\,EQ}$ are graphically estimated. R_{EQ} and $\sigma_{mean\,EQ}$ behave just like a hydrostatic stress ratio and hydrostatic mean stress in the process of the cyclic plastic-adaptation, respectively. This is due to the following reasons; (1) the irreversibility of expansion caused by cyclic plastic-adaptation and (2) the addibility of volume expansion which is produced under each principal cyclic stress. These two matters give the important hint to quantitative interpretation of cyclic plastic-adaptation; it is the potential described by Mises' equivalent stress that generates a driving force advancing cyclic plastic adaptaion and it is the algebraic sum of the maxmum value of principal stresses that provides the capability producing the cyclic plastic-adaptation. So, in the present study, in order to estimate the

potential at the notch root, Mises' equivalent stress concentration factor K_{teq} is defined by Eq. (1) where $\sigma_{xN},\cdots,\tau_{zxN}$ are the stress components of the nominal condition and $\sigma_{xNR},\cdots,\tau_{zxNR}$ are those of the notch root. Moreover, Eq. (2) that has been rewritten by principal stresses is obtained by dividing Eq. (1) with K_{teq}. Then, the principal stresses σ_{iNR} (i=1-3) are already not those arising actually at the notch root but those of which nominal values σ_{iN} (i=1-3) are expanded to the same potential level as the notch root has. After all, the principal stress of the un-notch condition where the potential is equal to that of the notch root is given by σ_{iNR} (i=1-3) in Eq. (3). The difference in the stress path of the nominal condition (magnified by K_{teq}) and the notch root condition is disregarded in the present method. As it is mentioned in the following section 2.3, such disregard does not affect the correspondence between fatigue strength of the notch and un-notch condition.

$$
\begin{aligned}
K_{teq} &= \frac{\sigma_{eq\,NR}}{\sigma_{eq\,N}} \\
&= \frac{\left(1/\sqrt{2}\right)\sqrt{\left(\sigma_{xNR}-\sigma_{yNR}\right)^2+\left(\sigma_{yNR}-\sigma_{zNR}\right)^2+\left(\sigma_{zNR}-\sigma_{xNR}\right)^2+6\left(\tau_{xyNR}^2+\tau_{yzNR}^2+\tau_{zxNR}^2\right)}}{\left(1/\sqrt{2}\right)\sqrt{\left(\sigma_{xN}-\sigma_{yN}\right)^2+\left(\sigma_{yN}-\sigma_{zN}\right)^2+\left(\sigma_{zN}-\sigma_{xN}\right)^2+6\left(\tau_{xyN}^2+\tau_{yzN}^2+\tau_{zxN}^2\right)}} \\
&= \frac{\left(1/\sqrt{2}\right)\sqrt{\left(K_{tx}\sigma_{xN}-K_{ty}\sigma_{yN}\right)^2+\left(K_{ty}\sigma_{yN}-K_{tz}\sigma_{zN}\right)^2+\left(K_{tz}\sigma_{zN}-K_{tx}\sigma_{xN}\right)^2+6\left(K_{tsxy}^2\tau_{xyN}^2+K_{tsyz}^2\tau_{yzN}^2+K_{tszx}^2\tau_{zxN}^2\right)}}{\left(1/\sqrt{2}\right)\sqrt{\left(\sigma_{xN}-\sigma_{yN}\right)^2+\left(\sigma_{yN}-\sigma_{zN}\right)^2+\left(\sigma_{zN}-\sigma_{xN}\right)^2+6\left(\tau_{xyN}^2+\tau_{yzN}^2+\tau_{zxN}^2\right)}}
\end{aligned}
\tag{1}
$$

$$
1=\frac{\sigma_{eq\,NR}}{K_{teq}\sigma_{eq\,N}}=\frac{\left(1/\sqrt{2}\right)\sqrt{\left(\sigma_{1NR}-\sigma_{2NR}\right)^2+\left(\sigma_{2NR}-\sigma_{3NR}\right)^2+\left(\sigma_{3NR}-\sigma_{1NR}\right)^2}}{\left(1/\sqrt{2}\right)\sqrt{\left(K_{teq}\sigma_{1N}-K_{teq}\sigma_{2N}\right)^2+\left(K_{teq}\sigma_{2N}-K_{teq}\sigma_{3N}\right)^2+\left(K_{teq}\sigma_{3N}-K_{teq}\sigma_{1N}\right)^2}} \tag{2}
$$

$$
\therefore\quad \sigma_{1NR}=K_{teq}\sigma_{1N},\quad \sigma_{2NR}=K_{teq}\sigma_{2N},\quad \sigma_{3NR}=K_{teq}\sigma_{3N} \tag{3}
$$

One example of the process of the cyclic plastic-adaptation at the notch root of material subject to cyclic torsion is shown in Fig.2, where plane stress is assumed. The segments *ab* and *cd* show the stress path of the nominal condition and the expanded one of the un-notch condition of which the potential is equal to the notch root, respectively. The segment *ef* shows the stress path where the

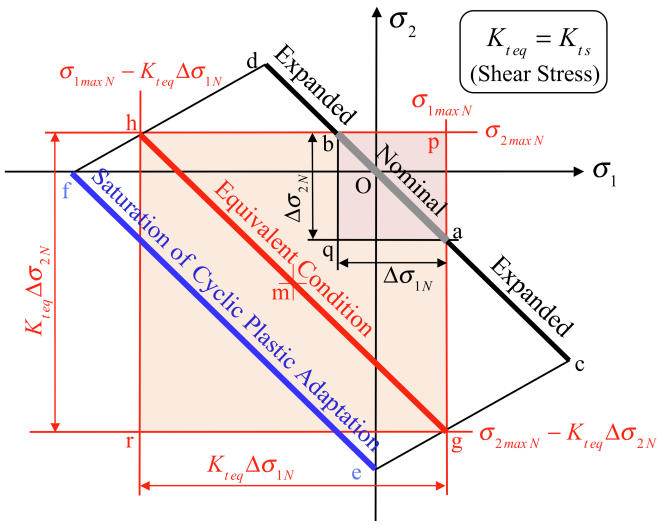

Fig. 2 Illustration of the graphic method of how to estimate R_{EQ} and $\sigma_{mean\,EQ}$ (cyclic torsion)

cyclic plastic-adaptation is accomplished completely. On the way of the cyclic plastic-adaptation process, as it is shown by the segment *gh*, each maximum values of the principal stress become equal to that of the nominal stress path, respectively. This is an important matter which should be mentioned specially; for, it means that, if the cyclic stress shown by the segment *gh* is applied to the un-notched material, the cyclic plastic-adaptation process at the notch root can be reproduced at the surface layer of the un-notched material. Therefore, it can be said that the segment *gh* corresponds to the equivalent cyclic stress condition between the notched and un-notched specimens. In the present study, the stress ratio R_N^* is newly defined for multi-axial stress condition other than the usual nominal stress ratio R_N. The R_N^* is formulated as a ratio of the algebraic sum of the x/y-coordinate value for each of the peak point *p* and *q* of the rectangle *paqb* with the line segment *ab* as a diagonal line (henceforth, the basic equations are shown with the three-dimensional form);

$$R_N^* = \frac{\left(\sigma_{1\,max\,N} - \Delta\sigma_{1N}\right) + \left(\sigma_{2\,max\,N} - \Delta\sigma_{2N}\right) + \left(\sigma_{3\,max\,N} - \Delta\sigma_{3N}\right)}{\sigma_{1\,max\,N} + \sigma_{2\,max\,N} + \sigma_{3\,max\,N}} \tag{4}$$

Next, the equivalent cyclic stress ratio R_{EQ} is formulated as the ratio of the algebraic sum of the x/y-coordinate values for each of the peak points *p* and *r* of the rectangle *pgrh* with the line segment *gh* as the diagonal line, and the expression is moreover simplified by using Eq. (4);

$$\begin{aligned} R_{EQ} &= \frac{\left(\sigma_{1\,max\,N} - K_{t\,eq}\Delta\sigma_{1N}\right) + \left(\sigma_{2\,max\,N} - K_{t\,eq}\Delta\sigma_{2N}\right) + \left(\sigma_{3\,max\,N} - K_{t\,eq}\Delta\sigma_{3N}\right)}{\sigma_{1\,max\,N} + \sigma_{2\,max\,N} + \sigma_{3\,max\,N}} \\ &= R_N^* - \left(K_{t\,eq} - 1\right)\left(1 - R_N^*\right) \end{aligned} \tag{5}$$

Last, the equivalent mean stress $\sigma_{mean\,EQ}$ is formulated as the algebraic sum of the x/y-coordinate values of the middle points *m* of the rectangle *pgrh* with the line segment *gh* as a diagonal line;

$$\begin{aligned} \sigma_{mean\,EQ} &= \left(\sigma_{1\,max\,N} + \sigma_{2\,max\,N} + \sigma_{3\,max\,N}\right) - K_{t\,eq}\left(\Delta\sigma_{1N} + \Delta\sigma_{2N} + \Delta\sigma_{3N}\right)\Big/2 \\ &= \left(\sigma_{1\,max\,N} + \sigma_{2\,max\,N} + \sigma_{3\,max\,N}\right) - K_{t\,eq}\left(\sigma_{1a\,N} + \sigma_{2a\,N} + \sigma_{3a\,N}\right) \end{aligned} \tag{6}$$

where, $\sigma_{i\,a\,N}$ (*i*=1-3) are the principal stress amplitude of the nominal condition. Saying again, R_{EQ} and $\sigma_{mean\,EQ}$ behave just like a hydrostatic stress ratio and hydrostatic mean stress in the process of the cyclic plastic-adaptation, regardless whether the stress components constituting them synchronizes or not, respectively. For the un-notch condition of $K_{t\,eq} = 1$, $\sigma_{mean\,EQ}$ of Eq. (6) is coincident with the mean hydrostatic stress that Sines introduced into his criterion [5].

2.3. Applicability of the R_{EQ}-ratio to fatigue strength diagramming

In order to prove the applicability of the equivalent cyclic stress ratio R_{EQ} and the equivalent mean stress $\sigma_{mean\,EQ}$, the fatigue strength of the specimen containing a comparatively large size notch (from the reason why influence of the notch size effect is little) is plotted on the diagram where the abscissa shows R_{EQ} and $\sigma_{mean\,EQ}$ and the ordinate does the notch root stress range $\Delta\sigma_{NR}$. Fig. 3 shows the fatigue test result concerning the notched and un-notched round-bar specimen of SM400 (low carbon structural steel) subject to cyclic axial loading under mean stress of tension side [1] and suject to rotating bending. Fig. 3(a) and (b) represent the R_{EQ}-based and $\sigma_{mean\,EQ}$-based fatigue strength diagram, respectively. The depth of the circumferential notch t is 3 *mm* for axial cyclic loading test and 1.5 *mm* for rotating bending test. The notch root radius ρ is changed in the range

from 0.1 to 3 *mm*. The R_{EQ} for axial cyclic load is estimated by FEM based on Mises' equivalent

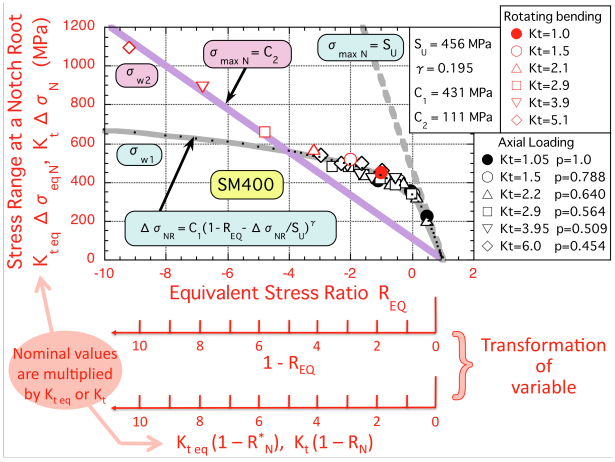

(a) R_{EQ} *vs.* $K_t\Delta\sigma_N$ diagram and similarity

(b) $\sigma_{mean\,EQ}$ *vs.* $K_t\sigma_{amp\,N}$ diagram and identity with that of the un-notch condition

Fig. 3 Fatigue strength diagram of SM400 steel round-bar specimen with the large-size notch (The fatigue tests were performed by cyclic axial load under mean stress [1] and rotating bending)

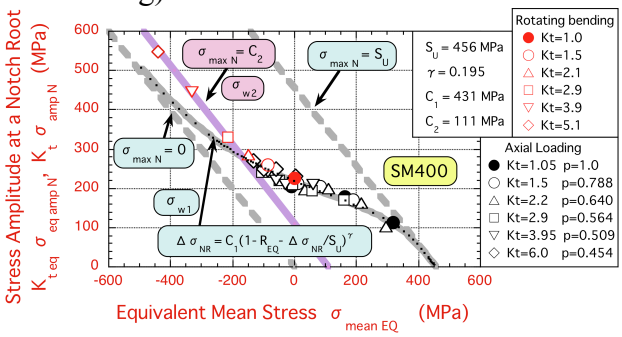

stress and the factor p done as the ratio of the average equivalent stress in the notch section $\bar{\sigma}_{eq}$ to the nominal stress σ_N [1]. In Fig. 3, the colored plot represents the experimental result. From the dispersion state of a plot, it is found, the fatigue strength is systematically arranged in spite of differences of stress concentration factors and mean stress, and it is clearly separable into the two groups of σ_{w1} and σ_{w2}. The curved and straight lines represent the fatigue strength diagrams of σ_{w1} and σ_{w2}, respectively, and they are drawn on the basis of the regression equations derived in the following chapter. The horizontal axis of the graph in Fig. 3(a) can be converted from the scale of R_{EQ} to the scale of $K_{t\,eq}\left(1-R_N^*\right)$ and $K_t\left(1-R_N\right)$ as shown in the lower berth of the graph;

$$1-R_{EQ}=K_{t\,eq}\left(1-R_N^*\right)=K_{t\,eq}\left(\Delta\sigma_{eq\,N}/\sigma_{eq\,max\,N}\right)=\Delta\sigma_{eq\,NR}/\sigma_{eq\,max\,N} \quad \text{(for axial load)} \quad (7)$$

$$1-R_{EQ}=K_t\left(1-R_N\right)=K_t\left(\Delta\sigma_N/\sigma_{max\,N}\right)=\Delta\sigma_{NR}/\sigma_{max\,N} \quad \text{(for rotating bending)} \quad (8)$$

Both the axes of the graph take the scale proportional to K_t. Therefore, it can be said that a similitude relation between the diagrams is materialized. This means that R_{EQ} is very useful as the correspondence parameter between the fatigue strength of the notched and un-notched specimen. The coincidence of a diagram in Fig. 3(b) means that the $\sigma_{mean\,EQ}$-based fatigue strength diagram obtained from the fatigue data of the notched specimen turns into the $\sigma_{mean\,N}$-based fatigue strength diagram of the un-notched specimen as it is.

3. Formulation of the fatigue strength diagram based on the R_{EQ}-ratio

3.1. Characterizing and mapping of the notch behavior

The notch is characterized by two parameters of ρ/t and $\sqrt{\rho t}/L_0$ as shown in Fig. 4(a) and (b), where the notch depth t and the notch root radius ρ are expressed as the co-ordinates after normalized by the size L_0. L_0 is introduced as an index for judging large size or small size notch. In the present study, $L_0=1mm$ is set emprically. The parameter ρ/t shows the sharpness of the notch which K_t depends on and the parameter ρt does the scale of the notch which the size effect depends on. Taylor classified the character of the notch behavior into three and drew the

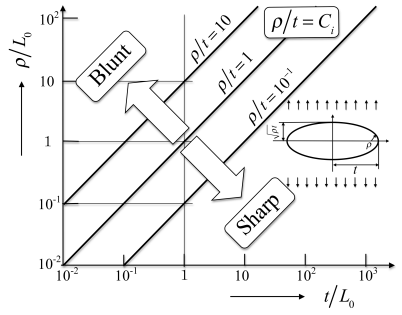

(a) Notch sharpness: ρ/t

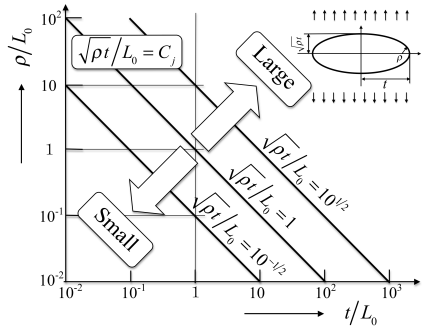

(b) Notch size scale: $\sqrt{\rho t}/L_0$

Fig. 4 Index parameter of notch sharpness and notch size scale: ρ/t and $\sqrt{\rho t}/L_0$

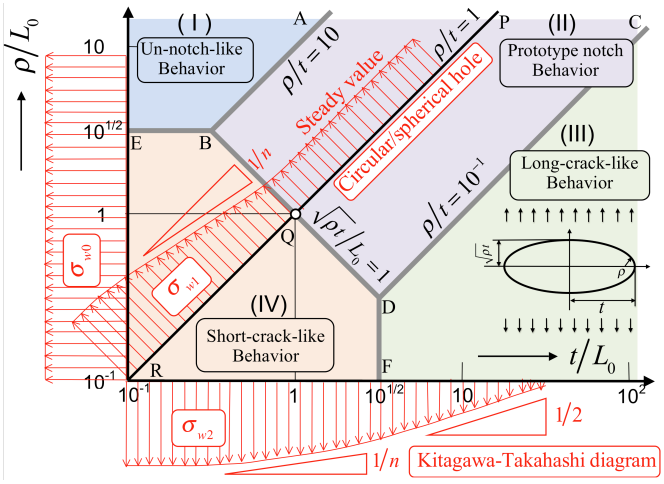

Fig. 5 Notch behavior map and a few typical distributions of fatigue strength threshold stress

distribution map on the key map [6]. His map seems to be rather suitable for expressing the characteristic of the fatigue strength σ_{w2}. So, a new map is created so that it can express the characteristic of the fatigue strength inclusive of the fatigue strength σ_{w1}. The new map is shown in Fig. 5, where the character of the notch behavior is classified into four domains; (I) Un-notch-like behavior, (II) Prototype notch behavior, (III) Long-crack-like behavior and (IV) Short-crack-like behavior. The four domains are partitioned with three characteristic lines AB, CD and BD and with the outgoing lines BE and DF drawn in the horizontal and perpendicular directions from the two intersections. The characteristic lines AB, CD and BD are expressed by the following simple formulas, $\rho/t=10$, $\rho/t=10^{-1}$ and $\sqrt{\rho t}/L_0=1$, respectively. A straight line PR formulated as $\rho/t=1$ expresses the size change of the circular or spherical hole that represents typical notch behavior. The distribution of the fatigue strength can be diagramed in a logarithmic scale by taking the z-axis in the direction perpendicular to space of the map. Three examples are schematically shown in Fig. 5. One is the diagram of the fatigue strength σ_{w1} for the circular or spherical hole. The diagram makes $\sqrt{\rho t}/L_0$ a variable and it is shown as a $\sigma_{w1}-\sqrt{\rho t}/L_0$ diagram on the line where $\rho/t=1$. As mentioned later, a $\sigma_{th}-\sqrt{area}$ diagram that makes Murakami's parameter of $\sqrt{area}$ a variable is a particular case of the $\sigma_{w1}-\sqrt{\rho t}/L_0$ diagram where $\rho/t=1$ and $\sqrt{\rho t}/L_0<1$. Another is Kitagawa-Takahashi diagram that makes a crack length a/a_2 a variable and the diagram is known as a $\sigma_{th}-a/a_2$ diagram [7]. The $\sigma_{th}-a/a_2$ diagram is depicted as a $\sigma_{w2}-t/L_0$ diagram on the horizontal axis (x-axis) in Fig. (5) where the crack length a/a_2 is replaced by the notch depth t/L_0. Moreover, Kitagawa and Takahashi prepared another critical size a_1 that represents the substantial transition from large size crack to small size one. This type of transition size on the fatigue strength σ_{w2} is expressed by replacing a_1/L_0 by t_0/L_0; the transition notch size is shown as $t_0/L_0=10^{1/2}$ in Fig. (5). The third is the fatigue strength of the un-notch condition σ_{w0} that is distributed on the vertical axis (y-axis) as a uniform value. This value is thought to be materialized in common where both ρ/L_0 and t/L_0 are extremely small.

3.2. Primary equations at the onset of formulation and their modification (Domain II)

The fatigue strength diagram is formulated first for the prototype notch of the domain II ($\sqrt{\rho t} \geq L_0$), where the notch size effect is not taken into consideration. In the following section 3.3, the equation is developed into a general form including the short-crack-like notch of the domain IV ($\sqrt{\rho t} < L_0$), where the notch size effect is taken into consideration. Primary equations that become a starting point of formulation are as follows, where Eq. (9) is quoted from Ref. [8];

$$\left(\Delta\sigma_{NR}\right)_{w1} = C_1\left(1-R_{EQ}\right)^{\gamma}, \qquad \text{(Fatigue strength } \sigma_{w1}\text{)} \tag{9}$$

$$\left(\Delta\sigma_{NR}\right)_{w2} = C_2\left(1-R_{EQ}\right). \qquad \text{(Fatigue strength } \sigma_{w2}\text{)} \tag{10}$$

Eq. (10) is rewritten by using the conversion expression of Eq. (8), as follows;

$$\left(\sigma_{max\,N}\right)_{w2} = C_2. \qquad \text{(Fatigue strength } \sigma_{w2}\text{)} \tag{11}$$

Eq. (12) is adopted as an asymptotic equation of Eq. (9) on σ_{w1}, so that the ultimate strength of material S_U may be gradually approached with an increase of the value R_{EQ};

$$\left(\sigma_{max\,N}\right)_{w1} = S_U \quad \text{i.e.} \quad \left(\Delta\sigma_{NR}\right)_{w1} = S_U\left(1-R_{EQ}\right). \tag{12}$$

Solving Eqs. (9) and (12) about $\left(1-R_{EQ}\right)$ and susequently transposing those algebraic sum to new $\left(1-R_{EQ}\right)$, Eq. (13) can be expressed;

$$\left(\Delta\sigma_{NR}\right)_{w1} = C_1\left\{1-R_{EQ}-\frac{\left(\Delta\sigma_{NR}\right)_{w1}}{S_U}\right\}^{\gamma}. \qquad \text{(Fatigue strength } \sigma_{w1}\text{)} \tag{13}$$

Eq. (13) is a very important as the expression which not only improves the precision for calculating the fatigue strength σ_{w1} but also explains how the tensile strength of material S_U relates quantatively with σ_{w1}. The equation expresses that the SCF-criterion (K_t-criterion) is materialized for σ_{w1} by using the equivalent cyclic stres ratio R_{EQ}. On the otherhand, for the fatigue strength σ_{w2}, Eq. (10) and (11) is used in a form as it is. It should be noted that, at this stage, γ, C_1 and C_2 are not material constants but variables. Strictly speaking, C_1 includes free boundary correction and C_2 includes a function of the notch depth t.

3.3. The equations generalized by incorporation of notch-size effects (Domain IV)

The factor of a notch size effect is incorporated into the euations derived in the foregoing paragraph. The judgement whether it is necessary to take the notch size effect into consideration or not is performed according to the value of a notch size $\sqrt{\rho t}$. In the present study, the value of $\sqrt{\rho t} = L_0$ is selected as the critical value as shown in Fig. 5. As it is mentioned in the foregoing section 3.1, the fatigue strength σ_{w1} depends on the notch size $\sqrt{\rho t}$ and the fatigue strength σ_{w2} does on the notch depth t. Therefore, the size factors F_{S1} and F_{S2} are introduced in the forms of the functions of $\sqrt{\rho t}$ and t, respectively;

$$F_{S1} = f_1\left(\sqrt{\rho t}\right), \tag{14}$$

$$F_{S2} = f_2\left(t\right). \tag{15}$$

Generally, the nominal stress of the plate and round-bar specimen containing a hole, a defect and a pre-crack is shown by gross-sectional stress. On the other hand, that of the plate and round-bar specimen containing an edge and circumferential notch is shown by net-sectional stress. These specimens are often furnished with the net-sectional area unified for different K_t and accordingly their gross-sectional area is different every specimen. Such difference has serious influence for the asymptotic process ofthe fatigue strength σ_{w1} to the ultimate strength of material S_U. So, a factor of F_G is introduced for the fatigue strength σ_{w1} expressed by the net-sectional stress, as follows;

$$F_G = A_{G0} / A_G\ , \tag{16}$$

where, A_{G0} and A_G are the gross-sectional area for $\sqrt{\rho t} = L_0$ and $\sqrt{\rho t} < L_0$, respectively. Also, it should be noted that the fatigue strength σ_{w2} in torsion is not subjected to the influence of the notch depth t. A concrete form of the function of F_{S1}, F_{S2} and F_G is summarized in Table 1. By using these factors, Eq. (9) and (12) are rewritten for the σ_{w1} as Eq. (17) and (18), respectively;

$$F_{S1}\left(\Delta\sigma_{NR}\right)_{w1} = C_1\left(1-R_{EQ}\right)^{\gamma}, \tag{17}$$

$$F_G\left(\sigma_{max\,N}\right)_{w1} = S_U \quad \text{i.e.} \quad F_G\left(\Delta\sigma_{NR}\right)_{w1} = S_U\left(1-R_{EQ}\right). \tag{18}$$

Eq. (18) is adopted as an asymptotic equation of Eq. (17) so that the ultimate strength of material S_U may be gradually approached with an increase of the value R_{EQ}. The final equation on the fatigue strength σ_{w1} is obtained as follows;

$$F_{S1}\left(\Delta\sigma_{NR}\right)_{w1} = C_1\left\{1-R_{EQ}-\frac{F_G\left(\Delta\sigma_{NR}\right)_{w1}}{S_U}\right\}^{\gamma}. \tag{19}$$

Eq. (19) is obtained by solving Eqs. (17) and (18) about $\left(1-R_{EQ}\right)$ and subsequently transposing those sum to new $\left(1-R_{EQ}\right)$. The final equation for the fatigue strength σ_{w2} is shown as follows;

$$F_{S2}\left(\Delta\sigma_{NR}\right)_{w2} = C_2\left(1-R_{EQ}\right) \quad \text{i.e.} \quad F_{S2}\left(\sigma_{max\,N}\right)_{w2} = C_2\,, \tag{20}$$

Table 1 Summary of the notch size correction factors

σ_w	F	Center hole (Gross-sectional stress)		Edge/circumferential notch (Net-sectional stress)		Small-size defect
σ_{w1}	$\sqrt{\rho t}$	$\sqrt{\rho t} \ge L_0$	$\sqrt{\rho t} < L_0$	$\sqrt{\rho t} \ge L_0$	$\sqrt{\rho t} < L_0$	$\sqrt{area} < L_0$
	F_{S1}	$F_{S1} = 1$	$F_{S1} = \left(\sqrt{\rho t}\right)^{1/8}$	$F_{S1} = 1.12$	$F_{S1} = 1.12\left(\sqrt{\rho t}\right)^{1/8}$	$F_{S1} = \left(\sqrt{area}\right)^{1/6}$
	F_G	$F_G = 1$		$F_G = 1$	$F_G = \frac{A_{G0}}{A_G} = \left(\frac{d+2L_0}{d+2\sqrt{\rho t}}\right)^2$	$F_G = 1$
σ_{w2}	t	$t \ge t_0$	$t < t_0$	$t \ge t_0$	$t < t_0$	$\sqrt{area} < L_0$
	F_{S2}	$F_{S2} = t^{1/2}$	$F_{S2} = t^{1/7}$	$F_{S2} = 1.12t^{1/2}$	$F_{S2} = 1.12t^{1/7}$	$F_{S2} = \left(\sqrt{area}\right)^{1/7}$

Note 1) $L_0 = 1mm$.
2) $t_0 = \sqrt{10}\,L_0 = \sqrt{10}\,mm$.
3) A value of 1.12 means a free boundary correction (F_0).

where, γ, C_1, C_2: Material constants.

4. Regression analysis on the fatigue data currently introduced in literature

Eq. (19) and (20) are applied to the regression analyses of fatigue data picked up from literatures. It is confirmed whether the function form of the equation derived in the preceding chapter 3 is appropriate as a regression equation. A part of the result is described below. Fig. 6 shows the result of a rotating bending test of S45C annealed steel with a round-bar specimen containing a small drill-hole. In the experiment [9], the diameter of a hole d was changed in the range from 0.04 to 0.5 *mm* and the depth t changed from 0.04 to 1 *mm*. The fatigue strength σ_{w1} is shown as a function of $\sqrt{area}$ -parameter in Fig. 6. The plot represents the experimental result and the curve shows the calculated result from the regression equation. The horizontal line represents the strength level of an un-notched specimen σ_{w0} is calculated backward from the regression equation. It turns out that the regression equation fits the experimental result very well. Fig. 7 shows the result of a rotating bending test of S45C annealed steel with a round-bar specimen containing an extremely shallow circumferential-notch. In the experiment [10], the notch root radius ρ was changed in the range from 0.01 to 0.6 *mm* and the depth t changed from 0.005 to 1.5 *mm*. The fatigue strength σ_{w1} and σ_{w2} were measured and they were shown as a function of a stress concentration factor K_t in Fig. 7(a) and (b), respectively. The colored plot represents the experimental result and the colored thin curve/line shows the calculated result. The horizontal thick gray line represents the strength level of an un-notched specimen σ_{w0} calculated backward from the regression equation. The thick gray curve obtained by dividing σ_{w0} by K_t is drawn for reference. In both Fig. 7(a) and (b), it turns out that the regression equation fits the experimental result very well. The regression analysis using the proposed equation has applied to the fatigue testing result of the total

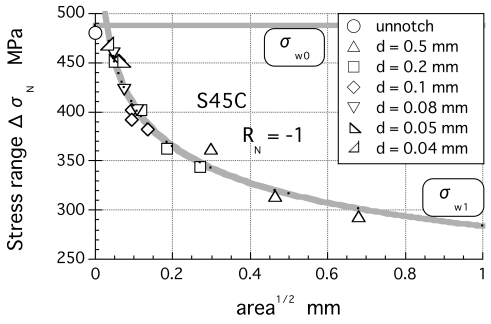

Fig. 6 Result of a regression analysis on rotating bending fatigue strength of S45C round-bar specimens containing small drill-holes (data from Ref. [9])

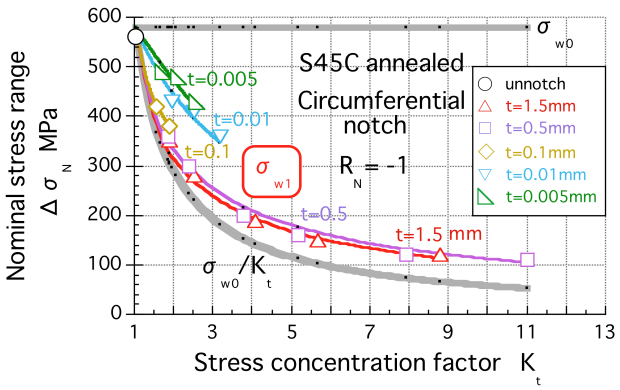

(a) Fatigue strength σ_{w1}

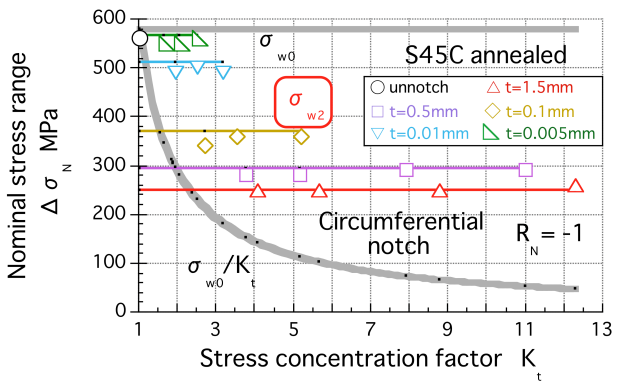

(b) Fatigue strength σ_{w2}

Fig. 7 Result of a regression analysis on rotating bending fatigue strength of S45C round-bar specimens containing small size circumferential notches (data from Ref. [10])

number of about 25 sorts of ferrous materials and their heat-treatment conditions in the present stage. As a result, it is found that the equation is materialized with less than 10% of error.

5. Conclusions

(1) A fatigue strength diagram is formulated and characterized as a function of the equivalent cyclic stress ratio (R_{EQ}-ratio). The R_{EQ}-ratio is derived from a hypothesis of cyclic plastic adaptation that reflects micro-mechanical behavior of a fatigue slip band.

(2) The graphic method estimating R_{EQ}-ratio based on the hypothesis of the plastic adaptation is developed in the present paper. R_{EQ}-ratio materializes a similitude relation between the fatigue strength diagrams of the notched and un-notched specimen in the case where the notch depth is comparatively large size of *mm*-order (where the notch size effect is negligible). It means that R_{EQ}-ratio can be applied as a main variable to the formulation of the fatigue strength diagram.

(3) The notch behavior is characterized and mapped by making the notch root radius and depth into variables. The notch size effect is systematically considered on the basis of the notch behavior map and the size effect factor is proposed for each of the fatigue strength σ_{w1} and σ_{w2}.

(4) The formulation of the fatigue strength diagram can be extended to the case of the extremely small size notch, such as the depth of 10 and 100 μm-order, where the size effect is dominant, and finally the generalized equations expressing the fatigue strength diagrams are proposed. These equations are applied to regression analyses on fatigue data of practically used metallic materials. As a result, it is found that the equations are materialized with less than 10% of error.

References

[1] H. Matsuno, Y. Mukai, A stress parameter for correspondence between notched and un-notched specimen fatigue data: strength of fatigue macro-crack initiation at a notch root in plates and round-bars, Proc. APSCFS & ATEM'01, JSME-MMD, Oct. 20-22, 2001, JSME No. 01-203, 394–399.

[2] U. Essmann, U. Gösele, H. Mughrabi, A model of extrusions and intrusions in fatigued metals, I. Point-defect production and the growth of extrusions, Phil. Mag. A, 44-2 (1981) 405–426.

[3] E.A. Repetto, M.A. Ortiz, A micromechanical model of cyclic deformation and fatigue-crack nucleation in f. c. c. single crystals, Acta Materialia, 45 (1997) 2577–2595.

[4] J. Polák, J. Man, K. Obrtlik, AFM evidence of surface relief formation and models of fatigue crack nucleation, International J. Fatigue, 25 (2003) 1027–1036.

[5] G. Sines, Failure of materials under combined repeated stresses with superimposed static stresses, Tech. Note 3495, National Advisory Committee for Aeronautics, Washington, DC, (1955).

[6] D. Taylor, A Mechanistic Approach to critical-distance methods in notch fatigue, Fatigue Fract. Engng Mater. Struct., 24 (2001) 215–224.

[7] H. Kitagawa, S. Takahashi, Fracture mechanics approach to very small fatigue crack growth and to the threshold condition, Trans. JSME. A, 45, 399 (1979) 1289–1303.

[8] H. Matsuno, A new interpretation of notch-sensitivity in fatigue of metals, Proc. 9-th International Fatigue Congress, May 14-19, 2006, Atlanta, Georgia, USA.

[9] Y. Murakami, M. Endo, A geometrical parameter for the quantitative estimation of the effects of small defects on fatigue strength of metals, Trans. JSME, A, 49, 438 (1983) 127–136.

[10] H. Nisitani, M. Endo, Unifying treatment of notch effects in fatigue, Trans. JSME, A, 51, 463 (1985) 784–789.